Measurements of Vehicle Glow on the Space Shuttle

S. B. Mende* and R. Nobles†
Lockheed Palo Alto Research Laboratory, Palo Alto, California
P. M. Banks‡
STAR Laboratory/SEL, Stanford University, Stanford, California
and
O. K. Garriott§ and J. Hoffman¶
NASA Johnson Space Center, Houston, Texas

From the combined data set of glow observations on STS-3, STS-4, and STS-5, some of the properties of the Shuttle glow were observed. Comparison of the STS-3 (240 km) and STS-5 (305 km) photographs show that the intensity of the glow is a factor of about 3.5 brighter on the low altitude (STS-3) flight. In an experiment on STS-5 the dependence of the intensity on the angle of incidence between the spacecraft surface normal and the velocity vector was observed. For a relatively large angle between the velocity vector and the surface normal there is an appreciable glow, provided the surface is not shadowed by some other spacecraft structure. The grating experiments (STS-4 photography only, STS-5 image intensifier photography) provided preliminary low resolution spectra of the spacecraft glow. Absolute intensity calibration of the instrument was also performed by means of a laboratory standard source. The glow amounted to a few hundred Rayleighs per Angstrom with a spectrum rising towards the infrared. This rise in intensity was not detected directly, but rather is an interpretation of the apparent spectrally uniform photographic spectrum, combined with the responsivity of the device, which falls rapidly in sensitivity towards the infrared. The integrated amount of vehicle glow emission in the passband of the instrument was of the order of several hundred kilorayleighs.

Introduction

The apparent vehicle glow of the Space Shuttle was detected during the flight of STS-3.[1] Although the Shuttle glow was not specifically predicted in advance of the flight, it has now been associated with other spacecraft glow which has been shown to surround free flier satellites such as the Atmospheric Explorer.[2,3] Specific investigation of the Shuttle glow was started on STS-4, when a transmission grating was mounted in front of a photographic camera and several exposures were taken on orbit to make preliminary spectral measurements.[4] The STS-4 experiment yielded a single 400-exposure photograph with glow spectral information. This image, obtained with relatively poor aspect with respect to the velocity vector, showed that the glow was observed predominantly in the far red to infrared region (6300-8000 Å) of the instrumental band pass (4300-8000 Å).

From the STS-4 investigation, it was evident that the intensity of the glow was reduced for higher altitude flights (STS-4 was at an altitude of 300 km, whereas STS-3 was at 240 km) and that relative insensitivity of unaided photography would seriously limit the spectral glow investigations. Because of this, on STS-5 a second instrument was used, an image intensified camera, which made the low-intensity spectral components of the glow detectable.

Submitted July 7, 1983; revision received Nov. 1, 1983.

*Staff Scientist.
†Senior Staff Scientist.
‡Professor of Electrical Engineering.
§Scientist-Astronaut.
¶Mission Specialist.

Performance of the Image Intensifier on STS-5

The image intensifier obtained for the STS-5 flight was made and delivered (by VARO Inc., Garland, Texas, under the tradename of Noctron 5) in a fully packaged configuration. This device includes a 25-mm-diam, second generation (micro-channel-plate) image intensifier, a power supply with two AA size batteries, a coupling lens, and adapter rings for for 35-mm cameras. Since the 35-mm camera type used on the orbiter was a Nikon, Nikon bayonet type adapter rings were employed. With these rings a conventional Nikon camera could be converted simply by including the Noctron 5 between the lens and the camera body. A special hood and camera bracket was used to mount the camera in the port, aft flight deck window in the Shuttle. The starboard, aft flight deck window was used for a conventional Hasselblad camera with the 100-mm focal length lens at F/3.5. For the image-intensified Nikon photography a 55-mm focal length F/1.4 objective was used in front of the image intensifier.

The image intensifier was a new item for space flight and its suitability for the Shuttle flight environment had to be carefully evaluated. Several optical tests were also performed on the device prior to flight. The imaging qualities of the device were evaluated by taking photographs of the night sky and of familiar objects in darkness. Used when looking through the viewfinder of the 35 mm camera, the image intensifier could be used as a night vision aid, and relatively high-intensity pictures could be obtained under starlit scene conditions. The use of laboratory standard light source and a spectral filter established that a 1-s exposure generated fairly good density when the source brightness was equivalent to 400 Rayleighs. At full gain, one could see scintillations with the naked eye through the viewfinder due to individual photoelectron emissions from the photocathode. However, these scintillations could not be recorded on film. The dark

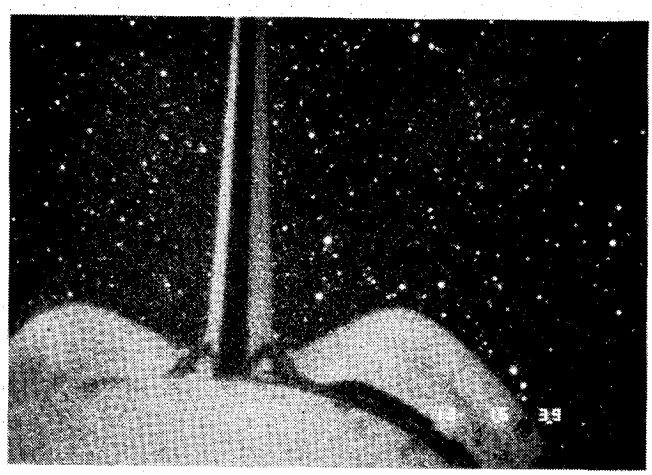

Fig. 1a Starfield taken by image intensified Nikon F/1.4 1/4 exposure on Tri-x film.

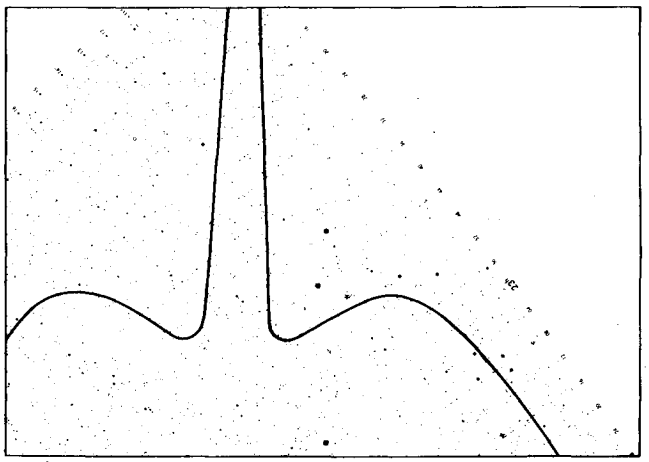

Fig. 1b Smithsonian Astrophysical Observatory star chart corresponding to the picture of Fig. 8a.

current performance of the device was particularly impressive. Made with the lens cap on, exposures of 10 s did not cause any noticeable increase in film density.

During the first half of the STS-5 glow experiment the image intensifier camera was used without the grating, and exposures were taken while the Shuttle was rolled about its axis to observe the change in glow intensity with respect to the velocity vector angle. During the interval while the velocity vector was underneath the payload bay, several starfield exposures were made. One of the best exposures was taken at 13:16:39. This exposure is shown in Fig. 1a. The luminosity on the Shuttle body is from starlight, as the Orbiter payload is essentially pointing away from the earth.

The starfield in the image is a section of the constellation Pegasus, the declination being a few degrees positive and right ascension around 23. The corresponding section of the star chart** is shown in Fig. 1b, together with a superimposed outline of the Shuttle. By counting the star images in a given area, one can identify all the stars presented on the chart. The chart includes stars down to 9th magnitude. This exposure was the shortest (¼s) of a group of three. On comparing Figs. 1a and 1b, the geometric fidelity of the instrument was seen to be excellent.

The image intensifier unit itself was not subjected to flight qualification testing, because a similar unit had already been qualified for the subsequent April 1983 STS-6 flight. All experiment hardware was stowed in stowage lockers during takeoff and landing.

**Smithsonian Astrophysical Observatory star chart.

Dependence of the Glow Intensity on the Angle of the Velocity Vector

Examination of the earlier glow photographs from STS-3 showed that only those surfaces which were in the direction of the velocity vector exhibited the glow phenomenon. An example of such a photograph is given on Fig. 2a. Figures 2a and 2b are the comparison of two similar pictures from STS-3 and STS-5, respectively. In both of these photographs, the velocity vector is pointing essentially from the port side in the upper hemisphere (photographs taken looking aft toward the vertical stabilizer and engine pod structures).

One of the objectives of the STS-5 experiment was to verify that the glow intensity depends solely on the attitude of the surface with respect to the velocity vector, and not on such parameters as the length of time during which the Shuttle was in the night side of the orbit, the amount of residue present on the photo-excited surfaces, or the amount of materials present due to venting or jet firings. It was also desirable to investigate, if possible, the dependence of the glow intensity on the angle of the velocity vector and the surface normal exhibiting the glow luminosity.

These objectives were achieved by the performance of the following experiment. During a nightside pass, a full > 360 deg roll was executed about the Shuttle x axis while the orbital velocity was approximately in the Shuttle y-z plane. (Conventional Shuttle coordinate system puts the x axis forward toward the nose, the y axis starboard and the z axis straight down through the floor of the payload bay.) During the experiment photographic sequences were taken of the vertical stabilizer surfaces as a function of the direction of the velocity vector. Sequences consisted of three exposures taken with the image intensifier with durations of 4 s, 1 s, and ¼ s, respectively. Simultaneously, photographs were taken with the unintensified Hasselblad camera, which was mounted in the other aft flight deck window. Of these only the longest (100-s) exposure from this camera gave acceptable photographic densities. However, during this long exposure, the attitude changed considerably, making the interpretation almost impossible. Thus, only the intensified images have been used in the analysis.

The shortest (¼-s) exposure produced the best intensified glow images, and hence these were used to obtain the results which are presented in Fig. 3.

The roll experiment started just prior to the taking of the first picture at 16 h and 33 min Mission Elapsed Time (MET). The velocity vector at this time is out of the port and upward directions, as shown by the arrow. Two minutes later, at 16:35, the Shuttle has rolled and the velocity vector is now essentially at about 35 deg above the -y axis (port wing). This can be verified because one can see the shadowing caused by the engine pod on the port side. At 16:37 the velocity vector dipped below the horizontal (x-y plane) at about 50 deg, and there is only a faint glow remaining on the port side of the stabilizer. The pictures taken at 16:37 and 16:39 show no glow at all because the velocity vector is towards the bottom and all the surfaces to be photographed were shadowed. The 16:41 picture shows glow on the upper portion of the starboard side of the stabilizer, where it was just coming out of the shadow of the starboard engine pod.

On each image of Fig. 3, the approximate direction antiparallel to the velocity vector is indicated. The direction of the velocity vector was first calculated from Orbiter data. The time code on each picture is accurate only to within a minute, and therefore the accurate value of the direction of the velocity vector for each photograph had to be interpolated from the position of the stars. By using the frame taken at

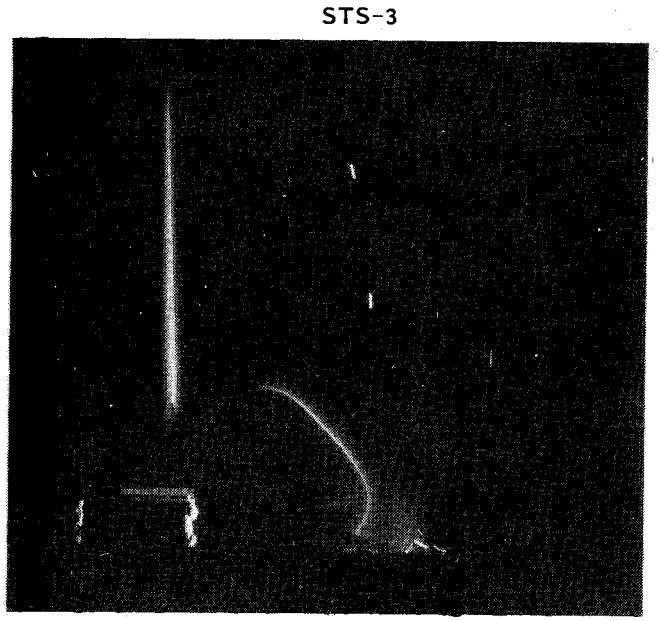

Fig. 2a Unaided Hasselblad photographs on STS-3 and STS-5, exposure times 10 and 100 s, respectively. The velocity vector is more or less from the same direction as Fig. 2b.

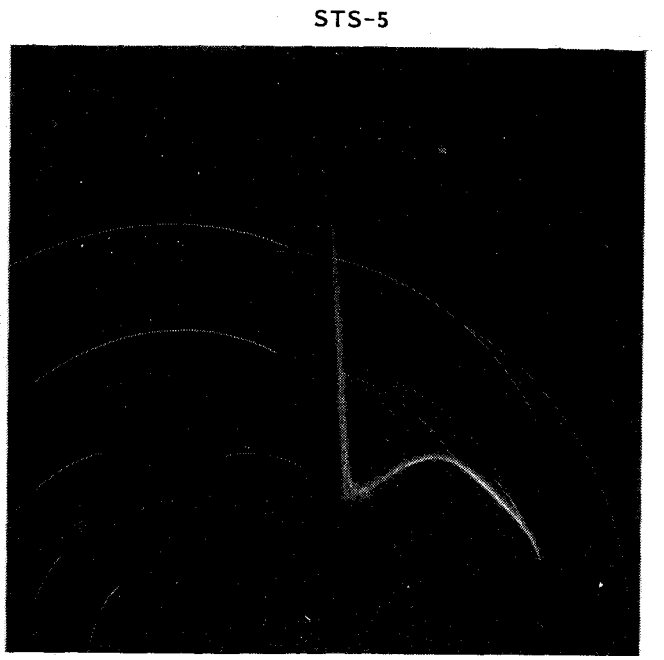

Fig. 2b Unaided Hasselblad photographs on STS-3 and STS-5, exposure time 100 s. The velocity vector is more or less from the same direction as Fig. 2a.

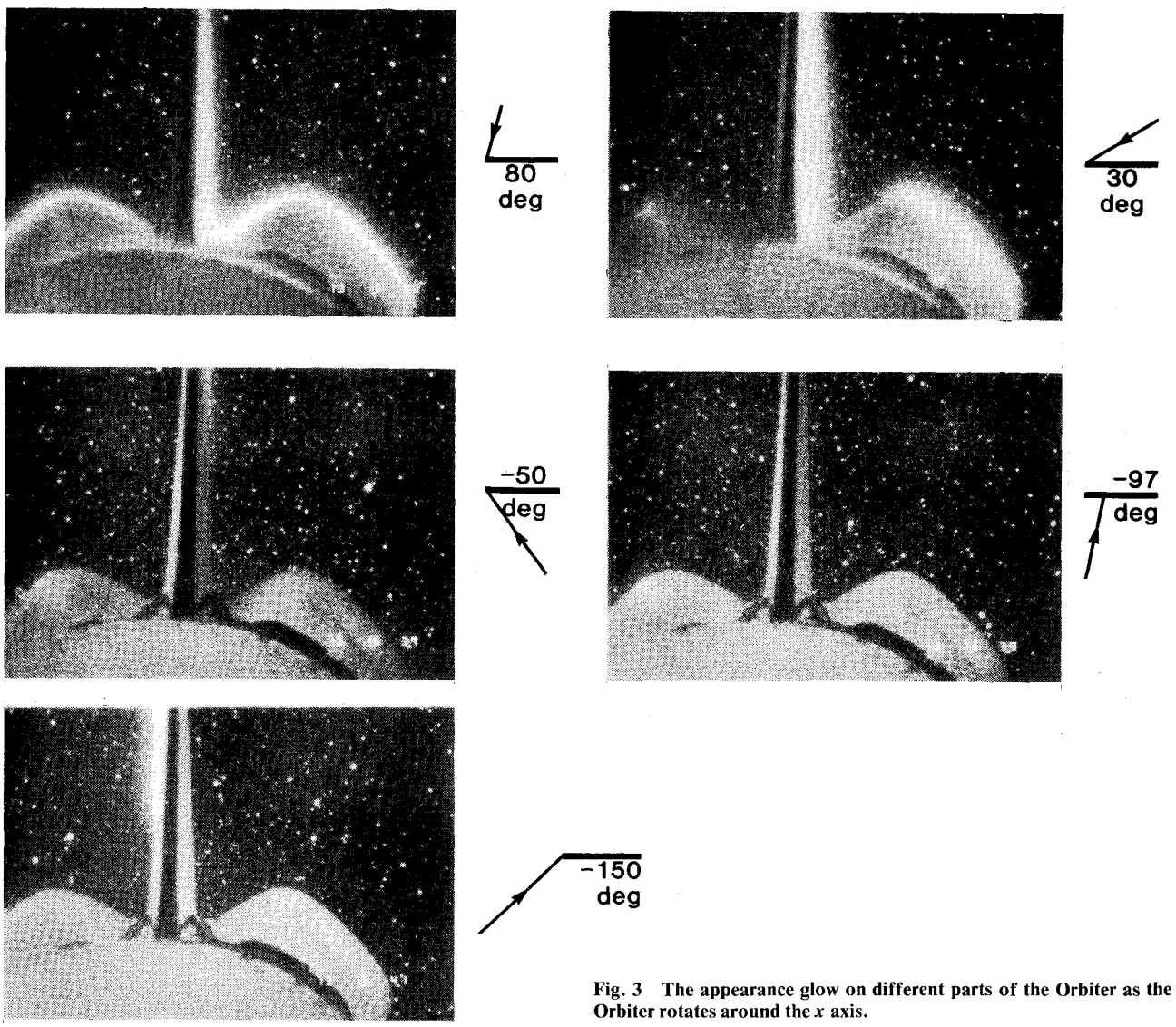

Fig. 3 The appearance glow on different parts of the Orbiter as the Orbiter rotates around the x axis.

16:35 MET, one can establish the direction of the velocity vector fairly accurately from the shadowing of the engine pod. By comparison with the Smithsonian Astrophysical Observatory Star Atlas, one can establish the rotation angle with respect to the stars for each exposure and the rotation angle for each exposure in the star coordinate system. Since the velocity vector was essentially in the y-z plane, the rotation of the stars gave a fairly accurate value for the angle of the velocity vector. Corrections had to be made for the change of the direction of the velocity vector due to the orbital motion, which amounted to approximately 4 deg per min.

The relative magnitude of the glow intensity could be obtained by the microdensitometering of the original negative films. Using the original negatives of the images presented on Fig. 2, tracings were made to measure the density of the glow luminosity on the tail section. This density was turned into equivalent exposure and the results are presented in Table 1.

Unfortunately, there are not enough data points to draw very solid conclusions. However, the numbers support the type of qualitative conclusions one was able to draw from the pictures. The system was calibrated for density vs exposure time, and from the measured density, the net relative exposure or intensity was derived. The intensity of the glow is not strictly proportional to the cosine of the angle and, therefore, not strictly proportional to the flux of incoming atmospheric constituents. It appears that very large angles between the surface normals and the velocity vector provide substantial glow. For example, in frame 13:16:33, the angle is 80 deg to the port side of the tail. When the angle decreases to 28 deg, the increase in glow is just a little over a factor of two. It would seem that the glow detected in the last frame (13:16:41) is anomalously too bright when compared to the frame taken at 13:16:35. However, the explanation is clear when one examines the actual photographs of Fig. 3. The glow on the starboard side is viewed tangentially, presenting a much narrower, and, therefore, brighter profile than on the port side, where the glow is visible over a larger region of the tail surface. If one were to integrate the glow over the larger region, no doubt the overall intensity would be of the same order as the more tangential view of the starboard side for the same velocity vector incidence angle. The comparison between the two sides is clearly dependent on the detailed geometry of the problem and we have not sufficient data to pursue this in greater detail.

Comparison of the STS-3 and STS-5 Glow Intensities

The glow was discovered by the analysis of the STS-3 photographs. On STS-4 a grating was used in front of the camera to obtain the spectra of the glow, but no grating pictures were taken for intensity comparisons. Nevertheless, it was suspected that the intensity of the glow was substantially lower on STS-4 than on STS-3. The altitude of STS-4 and STS-5 was close to 300 km, whereas the altitude of STS-3 was 240 km. If the glow were proportional to the density of atomic 0, one would expect to see a difference of approximately a factor of three in glow intensity due to altitude. On STS-5 the Hasselblad camera sequence was repeated in order to generate pictures for intensity comparisons with those of STS-3.

A relatively good comparison is provided in Fig. 2, where an STS-3 and an STS-5 photograph are presented side by side. In these pictures, the direction of the velocity vectors are similar.

Both photographs were taken by the same type of camera, a Hasselblad, and with the same type of lens, F/3.5. Both negative originals were processed similarly, and a control exposure wedge was used to obtain the exposure density curve of each flight film. On the STS-3 picture there are other light sources on the pallet besides the glow. Nevertheless, the glow is clearly visible on the side of the tail section and port engine pod.

From the comparison of the two photographs of Fig. 2, one can see that the glow generated density is roughly the same. This was confirmed by taking a microdensitometer trace of both images using the original negatives. However, the exposure durations for the STS-3 and STS-5 photographs were 10 and 100 s, respectively. This suggests a brightness ratio of the order of 10. In reality, however, the films exhibit reciprocity failure and the equivalent exposure is not directly proportional to the exposure time. Using measured reciprocity data[5] correction was made for the film reciprocity failure to obtain the real ratio of the glow intensities. The best estimate of the real intensity ratio between the STS-3 and STS-5 glow is about 3.5. This value is consistent with the decrease in atomic oxygen density for neutral gas pressure between the STS-3 and STS-5 flight altitudes.

Calibration of the Image Intensifier Grating Camera

To obtain an accurate wavelength scale, it is necessary to take into account several facts. Theoretically, the wavelength is only approximately proportional to the displacement of the image. In practice, both the lens and the image intensifier are likely to exhibit some geometric distortion. To minimize the errors, calibration photographs were taken of a slit illuminated by a mercury lamp. For these test exposures, the image intensifier camera system was in its full flight configuration. These images were microdensitometered to obtain the displacement due to each mercury line. The following mercury lines could be identified; 4047, 4358.4, 4916, 5460.7, and 5790.7 Å. Another line seen in the infrared was assumed to be the second order of 4047, thus equivalent to 8094 Å. To fit the best function for wavelength in terms of displacement, a least squares fit technique was used, where the wavelength y is a function of the displacement x according to a simple power law:

$$y = a_0 + a_1 \times X + a_2 \times x^2 + \ldots a_n \times x^n$$

The fitting was performed for the simple linear case where $n = 1$, the quadratic case, and the cubic case.

In order to interpret the absolute intensity of the spacecraft glow and the airglow features, it was necessary to take some spectral response calibration exposures. A secondary standard calibration source was used as the test object for these test exposures. The light source contained a quartz halide lamp with ground quartz diffusers to provide an extended source of reasonably spatially uniform emissivity.†† The lamp was masked off so that only a 2-cm-wide slit was showing, and exposures were taken with the image intensifier camera and the grating in position. The resulting streak generated in the dispersion direction was microdensitometered. The Shuttle window transmission, as provided by the Johnson Space Center, is presented in Fig. 4. This window was not available to be included in the calibration test exposures.

To obtain the quantitative response of the image intensifier camera system, it was necessary to convert the film density obtained by the microdensitometer into relative exposures. This conversion was obtained by microdensitometering several frames of different exposure times to obtain a relationship between film density and relative exposure. The relative exposure scale was corrected for the film reciprocity. In order to obtain quantitative measurement of the brightness of any feature, the observed density of the feature was converted into relative exposure and then compared to the relative exposure obtained using the standard light source. The relative exposure is, therefore, an arbitrary, but linear, scale unit. Because of these multiple nonlinear conversions, the expected errors in the absolute calibrations are probably no less than 20% to 30%.

††This lamp was manufactured and calibrated by Prof. R. H. Ether of Boston College.

The spectral response of the grating intensifier camera device is shown in Fig. 5 in relative exposure per kilorayleighs per Angstrom as a function of wavelength.

From the above, it can be seen that the spectral response of the image intensifier camera system rises sharply from 4000 Å to about 5400 Å. It is a little puzzling as to why the response is not more uniform towards the blue. Starting above 6500 Å, the responsiveness of the image intensifier falls off quite rapidly towards the infrared. This is presumably due to the decreased quantum efficiency of its photocathode.

The performance of the image intensifier grating camera could also be derived from star spectra. The best such spectral image was obtained of Zeta Pegasus. The image density was sufficient to produce a reasonable microdensitometer trace. In Fig. 6, the trace of the first-order spectra of this object is shown. The trace was actually superimposed on the trace of the background adjustment to the star spectrum. On the same figure is also shown the known spectrum of Zeta Pegasus.[6]

Figure 6 shows very clearly the blue and spectral response limitation of the system. Although the spectrum of the star increases towards short wavelengths, the response of the intensifier camera system drops off quite sharply above 4000 Å. The spectral transmission of the spacecraft windows, shown earlier in Fig. 3, were included in these observations. However, that does not appear to have imposed a limitation.

The Spectra of the Glow

During the STS-4 mission, the spectrum of the glow was recorded by an unaided Hasselblad camera using the objective grating.[4] Based on evidence of a single photograph, the spectrum of the glow consisted of a relatively diffuse spectrum primarily at the infrared end of the visible spectrum. Although putting quantitative numbers on the glow spectrum was hard, it seemed to be most intense in the region between 6300 and the window cutoff at 8000 Å. Because of the lack of sensitivity of the unintensified F/3.5 camera and the unfavorable direction of the velocity vector, a long (400-s) exposure duration was required.

On STS-5, the intensified camera permitted the taking of short exposures. Unfortunately, the STS-5 spectral results are not useful because the direction of the velocity vector was unfavorable during the time the grating exposures were taken. An additional problem ws the presence of the Earth near the field of view, producing a strong unwanted background. The clearest example of the glow spectra from STS-5 is on frame 13:17:01, shown in Fig. 7a. Figure 7b is an illustration of the features in the photograph.

The velocity vector in the spacecraft frame of reference at the time the photograph was taken (illustrated at top of Fig.7b) was 16 deg to the port from the forward direction and 40 deg above the bay horizontal. The most intense glow is on the horizontal surfaces, such as the top of the engine pods. The zero-order image of the tail and pods is in the left half of the picture. The almost vertical slanted line cutting through this image is a high-order spectral image of the airglow layer of the Earth limb. This is shown as a dashed line on the tracing. The lack of stars shows that the solid Earth forms the background for the whole image. Perhaps the clearest first-order spectral image is produced by the starboard engine pod. This image is in the center of the picture. The port engine pod is also producing a first-order spectrum on the right. They are both illustrated on the tracing.

The relative orientations of the glow on the engine pods and the grating rulings are most unfavorable. The linear wavelength scale was placed against the tip of the zero-order starboard engine pod. One can see that the first-order image of the Shuttle glow seems to occupy a large spectral region from 5000 to 8000 Å. The appearance of the first-order image is fairly uniform and diffuse, showing hardly any spectral features. This appears to contradict the findings of the STS-4 experiment, where the diffuse region was found to spread only between 6300 and 8000 Å. This discrepancy can be resolved by inspecting the absolute value of the glow intensity in Table 2. The image intensifier camera system is much more sensitive in the green region than the film. The marked dropoff in the sensitivity of the image intensifier towards the red-infrared suggests that the apparently uniform airglow spectra is, in reality, strongly increasing towards the infrared.

Table 1 Relative intensity of the STS-5 stabilizer glow

Time code	Net relative exposure	Angle of Side	Velocity to surface normal	Cosine of angle
13:16:33	38	Port	80 deg	0.174
13:16:35	89	Port	28 deg	0.88
13:16:37	tail in shadow		−50 deg	
13:16:39	tail in shadow		−97 deg	
13:16:41	113	Starboard	29 deg	0.87

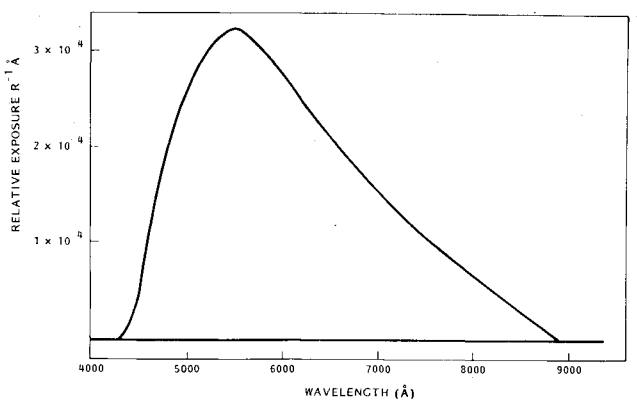

Fig. 5 Spectral response of the device in relative exposure (arbitrary units) per kilorayleighs per Angstrom as a function of wavelength.

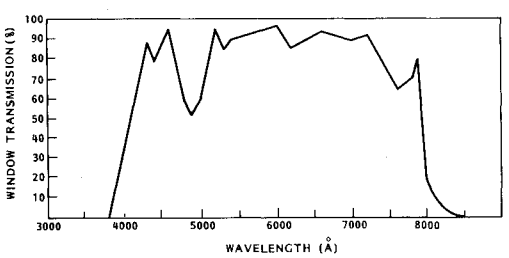

Fig. 4 Shuttle aft flight deck window transmission as provided by the Johnson Space Center. This window was not involved in the calibration test exposures.

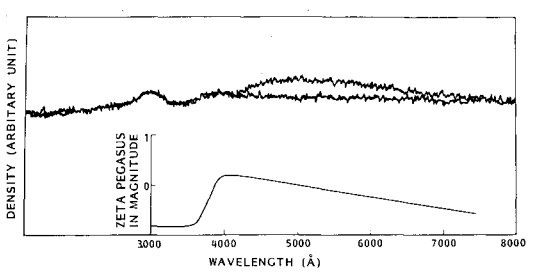

Fig. 6 Microdensitometer trace of Zeta Pegasus superimposed on the density trace of the background adjacent to the star spectra. The spectrum of Zeta Pegasus.

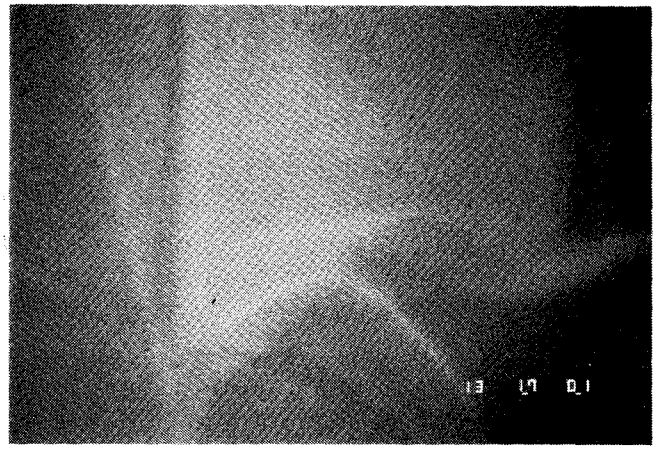

Fig. 7a A ½-s duration grating exposure of the Shuttle tail section with engine pods. The background is the atmospheric airglow emission.

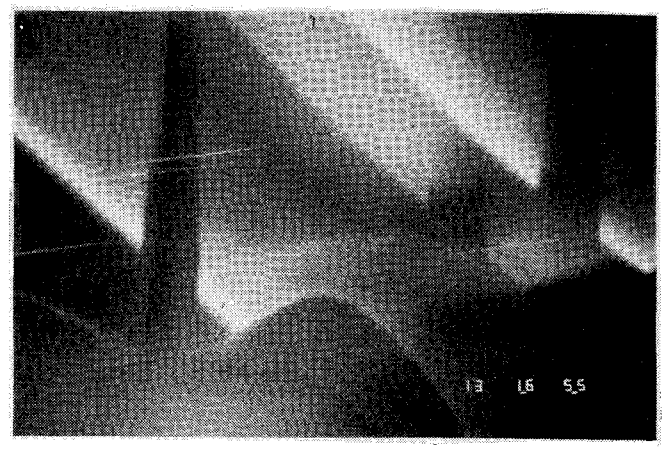

Fig. 8a The limb view of the Earth's airglow through the spectral grating. Image intensified Nikon with ½-s exposure. Objective is F/1. 4 55 mm.

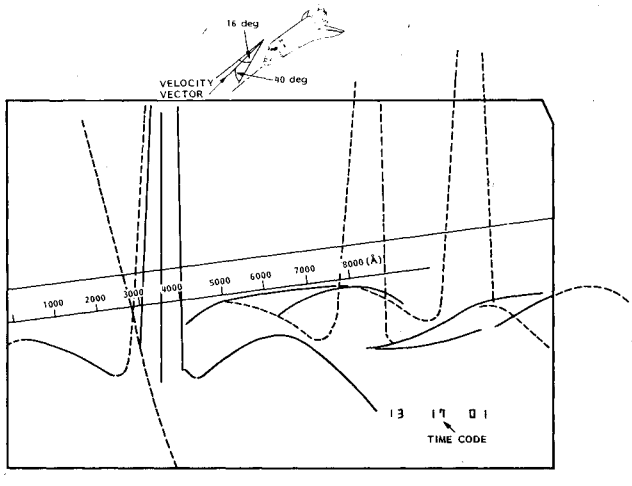

Fig. 7b Tracing of photograph of Fig. 7a. Velocity vector direction is indicated on top. Wavelength scale was superimposed on zero- and first-order images of starboard engine pod.

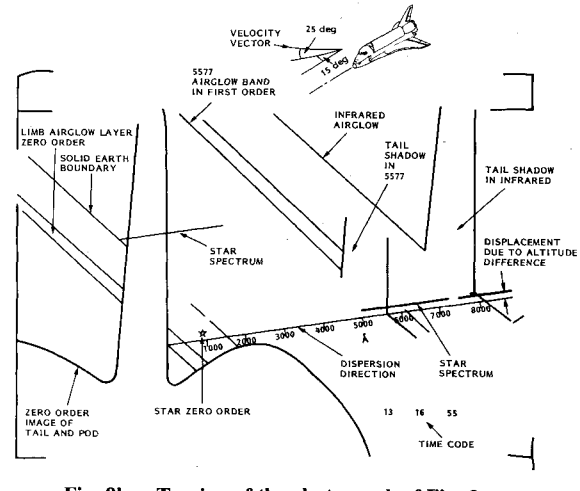

Fig. 8b. Tracing of the photograph of Fig. 8a.

On the STS-4 photographs, the blue-green region was still below the detection threshold, and only the more intense infrared end was detectable. Due to the adverse velocity vector angles and the diffusiveness of the glow spectra in these pictures, microdensitometer tracings did not produce any useful signals.

The device responsivity calibration using the intensity standard permits the interpretation of the various glow features in absolute quantities. The various features and the measured film densities and equivalent relative exposures are give in Table 2.

The Shuttle glow seems to spread through several thousand Angstroms so the total integrated amount may be as high as several hundred kilorayleighs in the visible regime alone.

Measurement of Airglow Emissions from the Shuttle Based Intensifier Camera

During the performance of the STS-5 glow experiment, some images of the Earth airglow were obtained. These photographs are the first Shuttle based images of this type and are, therefore, inherently valuable and, in addition, provide excellent calibration of the dispersion and spectral response of the image intensifier camera system.

One such image is illustrated in Fig. 8a. As illustrated in the tracing, Fig. 8b, the real or zero-order images are on the left. One can clearly see the tail and the two engine pods. The bright line running behind these Shuttle features down from left to right is the limb view of the Earth's atmosphere. Note that the Shuttle is oriented with the bay pointing downward because the image of the solid Earth occupies the top right three-quarters of the picture. The boundary of the solid Earth is faintly visible, as illustrated in the tracing of Fig. 8b. The zero-order (real) images of several stars are visible though the Earth's atmosphere.

The bright, narrow-streak, first-order images of stars show the dispersion direction of the grating. The zero-order images of most of these stars are actually outside the picture. There is one very bright star located between the port engine pod and the tail whose first-order spectrum is also visible on the picture.

There are some airglow bands which are parallel to the zero-order image of the limb airglow. The first one of these, going from left to right, is the 5577 Å atomic oxygen recombination glow. This emission is known to be a narrow emission line. Its thickness in first order is due to the altitude extent of the airglow layer. There is a dark band between this and the following wide diffuse region, which presumably corresponds to the gap between 5577 Å and the OH Meinel bands, starting at 6000. OH bands apparently decrease in intensity towards the infrared, which is attributed to the decrease in sensitivity of the device. Towards the infrared, the brightest airglow feature is found.

The Shuttle tail features intersect the airglow layer, causing repeated shadows in all the brighter airglow features. Thus, there is a tail shadow in 5577 and there is an even more distinct one in the infrared. The edges of the 5577 tail shadow are very sharp, showing that the 5577 Å line is, in fact, a very narrow spectral feature. Note that the tail, being a sharp edge, can be regarded as one half of the spectrometer slit, and, therefore, the resulting intensity change can be interpreted in first order as an accurate measure of the wavelength. This interpretation allows one to make spectral measurements independent of the spatial width of the emitting region. A linear wavelength scale was superimposed on the portside edge of the shadow of the tail section in Fig. 8b. The scale confirms that the first shadow is approximately at 5577 Å and the second shadow is near 8000 Å.

This scale also shows an interesting feature. The scale was carefully drawn parallel to the spectra of the stars to follow the dispersion direction. The scale was also drawn through the intersection of the top of the airglow layer (bottom left on figures) with the tail section. The scale goes through the corresponding intersection of the tail section with the 5577 image, but is slightly below the corresponding intersection in the infrared image. The explanation is that the infrared airglow layer is displaced in altitude from the 5577 airglow layer by about 20 km. Careful examination of Fig. 8a shows that the zero-order image of the airglow layer consists of two parallel features. This is most discernible towards the top left part of the zero-order image. The double layer of the airglow image and also be seen on other photographs of the limb airglow layer.[1,7]

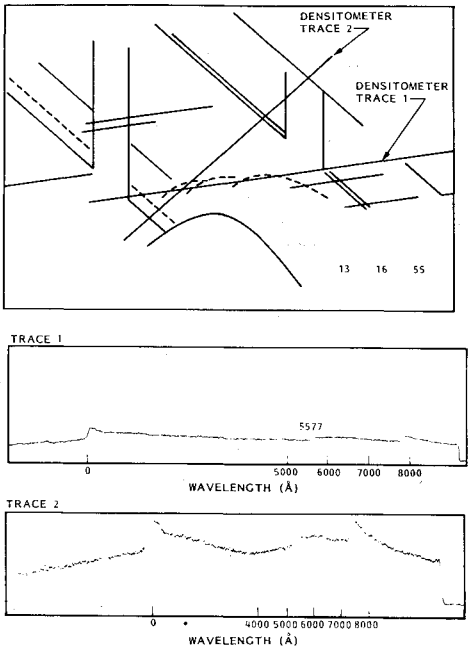

Fig. 9 The top panel indicates the two microdensity traces obtained from the original negative of Fig. 8a. The center panel shows the microdensity trace parallel to the dispersion direction through the tail section shadows.

The Shuttle and the velocity vector duration at the time of the exposure are illustrated at the top of Fig. 8b. The velocity vector duration was 15 deg towards starboard from the forward direction and 25 deg up in the bay frame of reference. This attitude to the velocity vector is relatively unfavorable from the point of view of strong glow production, but there is some weak glow on the port side engine pod and there are some faint images of the starboard engine pod in first order. These were indicated as dotted images in the figure.

In Fig. 9, the top panel indicates the location of the microdensity traces obtained from the original negative of photograph Fig. 8a. The middle panel shows the microdensity trace parallel to the dispersion direction through the tail section shadows. This density trace allows the wavelength scale to be determined most accurately. The bottom trace was obtained by tracing perpendicular to the airglow layer. This direction maximizes the signal-to-noise ratio, but distorts the wavelength scale and limits the wavelength resolution to the spatial width in the zero-order image. The intensities of the airglow features are given in Table 3.

The intensity values thus obtained agree very well with prior measurements. To compare to prior nonspectral measurements, it is necessary to convert these to total intensities in Rayleighs within the spectral band of interest.

The infrared airglow is spatially wider than its spectral bandwidth. To interpret the total emission, one must refer to the previous measurement of the bandwidth of the feature using the tail shadow. By so doing, one obtains roughly 40-60 Å, which puts the the intensity of the O_2 atmospheric band system at about 300 to 400 kR, in good agreement with previous oblique rocket measurements.[8]

Since the 5577 is a spectral line feature and its spectral width is very thin, the instrument's resolution (20-30 Å) needs to be taken into account. Thus the total measured 5577 intensity is 4000 to 6000 Rayleighs.

Table 2 Absolute calibration of various glow spectra

Frame I.D. (time code)	Feature description	Density (image)	Density (bckgd.)	Rel. Exposure (s)	Intensity Rayleighs/ Angstrom
13:17:01 (½ s)	Shuttle glow of starboard pod pod	1.08	0.96	0.086	(@ 7600 Å) 850 (@ 7000 Å) 500 (@ 6000 Å) 300

Table 3 Absolute intensity of the various air-glow emissions

			Background	Exposure	Intensity Rayleighs/ Angstrom
13:16:55 (½ s)	infrared airglow	1.50	1.17	00.56	(@ 7600 Å) 5000
13:16:55	green airglow	1.25	1.20	0.061	(@ 5577 Å) 200
13:16:55	OH continuum	1.17	0.95	0.050	(@ 7300 Å) 300

Values were obtained by dividing relative exposure by device responsiveness (see Fig. 4), as normalized to ½-s exposure.

The measured intensity of the OH band agrees quite well with other measurements[9] of the airglow if we account for the limb view intensification. Thus the spacecraft glow is at least equivalent to or brighter than the OH band in limb view. The intensity of the OH band also agrees quite favorably with the expected limb intensities.

Conclusions

From the combined data set of glow observations on STS-3, STS-4, and STS-5, it is possible to define some of the properties of the Shuttle glow. Comparison of the STS-3 and STS-5 photographs shows that the intensity of the glow is a factor of about 3.5 brighter on the low altitude (STS-3) flight. This result seems to be in good agreement with the ratio of atmospheric densities between the two altitudes. STS-3 was flown at an altitude of about 240 km, whereas STS-was flown at an altitude of 305 km. The Orbiter was purposely rotated about the x-axis in an experiment on STS-5 and the glow was observed. This experiment showed conclusively that the intensity of the glow strongly depends on the angle of incidence between the spacecraft surface and the velocity vector. The relationship does not appear, however, to be a simple cosine law dependence. For a relatively large angle between the velocity vector and the surface normal, there is an appreciable glow, provided the surface is not shadowed by some other spacecraft structure. As the angle becomes less, the glow intensifies. Unfortunately, the experiment did not provide sufficient data to express the exact mathematical relationship between the spacecraft glow intensity and the angle between the surface normal and velocity vector.

The grating experiments provided a preliminary, low-resolution spectra of the spacecraft glow. Accurate wavelength calibrations of the STS-5 instrument allowed a measurement of the spectrum and intensity of the Earth's airglow. Comparisons with prior airglow measurements provide confidence regarding the glow intensities obtained in the experiment. Absolute wavelength calibration of the instrument was also performed by means of a laboratory standard source. Within the spectral bandwidth of the experiment the dominant airglow line is the (0,0) band of atmospheric O_2. The limb intensity of this line is the order of 300 kilorayleighs.[8] Other prominent features are the 5577 Å line and the OH emission bands. The intensity of all these agree well with previous measurements and limb intensity predictions.

The spectra of the glow measurements on STS-5 were relatively unfavorable, due to the large angle between the velocity vector and the glowing surfaces and to the fact that the weak first-order spectrum was superimposed on the Earth's bright airglow. Nevertheless, a weak spectra was obtained which shows a spectrally uniform glow. The photographic densities due to this glow were measured and compared to the absolute intensity measurements. This glow amounted to a few hundred Rayleighs per Angstrom, with a spectrum rising towards the infrared. This rise is deduced from an apparent spectrally-uniform photographic spectrum combined with the responsiveness of the device, which is rapidly falling towards the infrared. The integrated amount of light in the passband of the instrument was of the order of several hundred kilorayleighs.

Acknowledgments

The authors would like to thank Mr. E. L. Michel for his efforts in doing all the necessary background work in getting the STS-4 and STS-5 experiments on the Shuttle. Many thanks are also due to the astronauts who have carried out the experiments in flight. We are grateful to the flight crew of STS-5, especially J. P. Allen and R. F. Overmayer, who operated the flight cameras. Helpful discussions with Dr. R. Peterson regarding microdensitometry and Prof. R. H. Eather regarding absolute calibrations are also gratefully acknowledged. This program was supported by NASA under Contract NASW-3658 and by a Lockheed Independent Research Program.

References

[1]Banks, P.M., Williamson, P.R., and Raitt, W.J., "Space Shuttle Glow Observations," *Geophysical Research Letters,* Vol. 10, Feb. 1983, p. 118.

[2]Torr, M.R., "Optical Emissions by Spacecraft-Atmosphere Interactions," *Geophyscial Research Letters*, Vol. 10, Feb. 1983, p.14.

[3]Yee, J.H. and Abreu, V.J., "Visible Glow Induced by Spacecraft-Environment Interaction," *Geophysical Research Letters,* Vol. 10, Feb. 1983, p.126.

[4]Mende, S.B., Garriott, O.K., and Banks, P.M., "Observations of Optical Emissions on STS-4," *Geophysical Research Letters,* Vol. 10, Feb. 1983, p.122.

[5]Lamar, N., Private Communications, 1983.

[6]Berger, M., Catalog of Spectrophotometric Scan of Stars, *Astrophysical Journal Supplement Series,* Vol. 32, Sept. 1976, pp. 7-78.

[7]Gariott, O.K., "Visual Observations from Space," *Journal of the Optical Society of America,* Vol. 69, Aug. 1979, pp. 1064-1068.

[8]Megill, L.R., Despain, A.M., Baker, D.J., and Baker, K.D., "Oxygen Atmospheric and Infrared Atmospheric Bands in the Aurora," *Journal of Geophysical Research,* Vol. 75, Sept. 1970, pp.4775-4785.

[9]Broadfoot, A.L. and Kendall, K.R., "The Airglow Spectrum, 3100-10,000 A," *Journal of Geophysical Research,* Vol. 73, Jan. 1968, p.426.